ARTICLES

Journal of Semiconductors
(2023) 44, 052802
doi: 10.1088/1674-4926/44/5/052802

JOS

Suitable contacting scheme for evaluating electrical properties of GaN-based p-type layers

Siyi Huang[1, 2, 3], Masao Ikeda[2, 3, †], Minglong Zhang[1, 2, 3], Jianjun Zhu[2, 3], and Jianping Liu[1, 2, 3, †]

[1]School of Nano-Tech and Nano-Bionics, University of Science and Technology of China, Hefei 230026, China
[2]Suzhou Institute of Nano-Tech and Nano-Bionics, Chinese Academy of Sciences, Suzhou 215123, China
[3]Key Laboratory of Nanodevices and Applications, Chinese Academy of Sciences, Suzhou 215123, China

Abstract: A suitable contacting scheme for p-(Al)GaN facilitating quick feedback and accurate measurements is proposed in this study. 22 nm p$^+$-GaN followed by 2 nm p-$In_{0.2}Ga_{0.8}N$ was grown on p-type layers by metal-organic chemical vapor deposition. Samples were then cut into squares after annealing and contact electrodes using In balls were put at the corners of the squares. Good linearity between all the electrodes was confirmed in *I*–*V* curves during Hall measurements even with In metal. Serval samples taken from the same wafer showed small standard deviation of ~ 4% for resistivity, Hall mobility and hole concentration. The influence of contact layer on the electrical characteristics of bulk p-type layers was then investigated by step etching technique using inductively coupled plasma etching and subsequent Hall-effect measurements. Identical values could be obtained consistently when a 28 nm non-conductive layer thickness at the surface was taken into account. Therefore, the procedures for evaluating the electrical properties of GaN-based p-type layers just using In balls proposed in this study are shown to be quick and useful as for the other conventional III–V materials.

Key words: GaN; electrical properties; ohmic contact

Citation: S Y Huang, M Ikeda, M L Zhang, J J Zhu, and J P Liu, Suitable contacting scheme for evaluating electrical properties of GaN-based p-type layers[J]. *J. Semicond.*, 2023, 44(5), 052802. https://doi.org/10.1088/1674-4926/44/5/052802

1. Introduction

After the realization of p-type conduction in Mg-doped GaN by Akasaki and Amano *et al.* with low-energy electron beam irradiation (IEEBI) treatment in 1989[1] and thermal annealing in N_2 ambient by Nakamura *et al.* in 1992[2], the studies on improving the electrical properties of GaN-based p-type layers have been carried out successively[3–10]. Hall-effect measurements are commonly used to evaluate electrical properties. A good ohmic contact is generally required to obtain accurate values during the measurements. High work function metal such as Pd[11–13] or Ni[14, 15] deposited in a high vacuum chamber is essential and special contact layers are usually adopted. It is time-consuming and much costly for the additional annealing of metal contact or the removal of contact layers for accurate measurements.

In this paper, a suitable contacting scheme consisting of p-InGaN and p$^+$-GaN was grown on GaN-based p-type layers. After the annealing of p-type layers, indium was used as the contact metal. The electrical properties could be evaluated quickly and accurately with such simple procedures. The use of the contact structure was proved experimentally to have no influence on the measurement of p-(Al)GaN layers.

2. Experiment methods

The GaN-based p-type layers and special contact layer were grown on *c*-plane free-standing (FS-) GaN substrates at atmospheric pressure in Taiyo Nippon Sanso (TNSC) horizontal MOCVD reactor (SR-4326KS). 1 μm-thick unintentionally doped GaN was grown on FS-GaN substrate at 1000 °C, followed by 500 nm Mg-doped p-GaN or p-$Al_{0.14}Ga_{0.86}N$ (2.5 nm)/GaN (2.5 nm) superlattices (SLs) and 22 nm heavily doped p$^+$-GaN grown at 850 °C. After that, temperature was lowered to 740 °C to grow 2 nm p-$In_{0.2}Ga_{0.8}N$. Trimethylgallium (TMGa), trimethylaluminum (TMAl), trimethylindium (TMIn), ammonia (NH_3) and bis-cyclopentadienyl magnesium (Cp_2Mg) were used as the precursors for Ga, Al, In, N, and Mg, respectively. Hydrogen (H_2) was used as a carrier gas when growing (Al)GaN layers while nitrogen (N_2) was used for InGaN layers. The Mg doping level in bulk p-type layers were less than 2×10^{19} cm^{-3}. Due to some delay in raising the doping level, 22 nm thick p$^+$-GaN was grown to raise the Mg concentration up to ~ 1×10^{20} cm^{-3}. The Mg doping concentration could be made ×11 times higher in 22 nm thickness. This rate was confirmed by secondary ion mass spectroscopy (SIMS) using another sample at a deeper position apart from the surface to avoid the measurement error due to surface contamination. The doping level of Mg in the top 2 nm p-InGaN layer was estimated to be 4×10^{19} cm^{-3} by the Mg and Group III mole flow ratio and SIMS results of separately grown thicker InGaN layers.

V-pits would form during the growth below the temperature around 850 °C through threading dislocations (TDs) for Mg-doped p-GaN layers[16]. FS-GaN substrates with low TDs were therefore used in this experiment to measure the electrical properties avoiding the V-pits formation. Common sap-

Correspondence to: M Ikeda, mikeda2013@sinano.ac.cn; J P Liu, jpliu2010@sinano.ac.cn
Received 28 OCTOBER 2022; Revised 29 JANUARY 2023.
©2023 Chinese Institute of Electronics

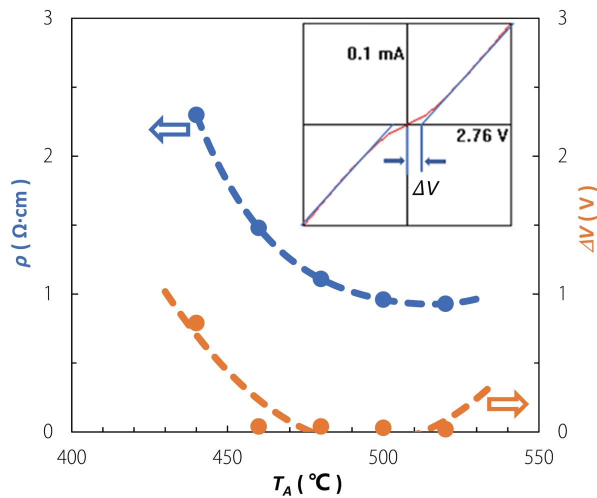

Fig. 1. (Color online) The effect of different T_A on the ρ and ΔV of Hall samples.

phire substrates can also be used when p-type growth temperature is higher than 900 °C which is also confirmed by our separate study.

Samples were annealed in a tube furnace in dry air at ~ 500 °C for 15 min to activate Mg in p-type layers. Then they were cut into 5 × 5 mm^2 squares and ϕ 0.2 mm indium balls were pressed near the corners of the squares (diameters of the indium platelet became ~ 0.6 mm after pressing). The samples were heated up to 300 °C for several seconds on a hot plate to make close contact between indium dots and contact layer. The diameters of the pressed indium platelets shrunk a little to ~ 0.4 mm after heating. Resistivity and Hall-effect measurements with van der Pauw geometry were performed by Accent HL8800 to obtain sheet resistivity (R_{sh}), resistivity (ρ), Hall mobility (μ) and hole concentration (p) at room temperature. The magnetic field was 0.388 T and the currents were 100 μA during the measurements.

Inductively coupled plasma (ICP) etching was carried out for selected Hall samples in an Apex SLR ICP system at 6.0 mTorr. The flow rate of boron trichloride (BCl_3) was 25 sccm and RF power was 55 W. Hall effects were measured again after ICP etching to check the influence of contact layer on the electrical properties of bulk p-type layers.

3. Results and discussion

Linear *I*–*V* curves are essential to obtain accurate results from Hall-effect measurements. Therefore, annealing temperature (T_A) ~ 500 °C was chosen to avoid the degradation of p-InGaN contact layer to make a good ohmic contact. Different annealing temperatures from 440 to 520 °C were checked for p-GaN samples. *I*–*V* curves from different electrodes were also examined during the measurements. As the *I*–*V* curve shows in the inset of Fig. 1, ΔV is defined as the linear intercept of bulk p-type layers with x (voltage) axis. It is obvious that smaller ΔV refers to better linearity. It should be noted that each data point in Fig. 1 is the average of 4 samples annealed at the specific temperature. Judging from the ρ and ΔV from Fig. 1, 460 °C was almost enough to get good ohmic contacts while ~ 500 °C was necessary to further remove H from the bulk p-layers. Although not shown here, it was also confirmed with other samples that the ΔV increased with increasing the annealing temperature above 520 °C, which is probably caused by the oxidization of top InGaN layer in an oxygen containing ambient. As a result, the annealing temperature was chosen to be 510 °C to acquire both good contacts and sufficient activation of p-layers.

After optimizing the annealing temperature, the electrical properties of p-GaN and p-AlGaN/GaN SLs can be easily measured. 8 samples were taken from each one quarter of 2 inch wafer. Fig. 2 shows the results for p-GaN and p-AlGaN/GaN SLs, respectively.

Good linearity was confirmed in *I*–*V* curves between all the electrodes and typical examples are shown in Fig. 2. *F* factors were 1.00 ± 0.01 in the measurements showing good symmetries. The solid lines are the average value of 5 samples in Figs. 2(b) and 2(c) and 7 samples in Figs. 2(e) and 2(f). The standard deviations of ρ, μ, p and R_{sh} were calculated to be ~ 3% for p-GaN samples and ~ 4% for p-AlGaN/GaN SLs samples. Not all the square samples could be measured because of the leakage due to pits or through side walls, the faults during cleavage of squares or the peeling off of soft In dots. Still more than 5 out of 8 samples showed consistent results. This is more than enough to get accurate data for p-type layers.

It's necessary to check the influence of the contact layer on the electrical properties of bulk p-type layers. Therefore, step etching was applied for further analysis. During the etching procedure, not only the surface layer will be removed but also some etching damage will penetrate into the surface region (Fig. 3). The damage was mainly caused by the formation of nitrogen vacancy (V_N) during ICP etching[17, 18]. V_N is a donor defect and can compensate a hole and also hazards to p-type conduction by forming Mg–V_N complexes in GaN-based materials. Different etching method leads to different etching damage, so it is meaningful to determine the etching damage thickness. It is obvious that relatively weaker etching conditions as we chose is preferred in this experiment.

Etching depth (d_E) was measured by AFM to determine ICP etching rate. Since the p-AlGaN/GaN SLs samples have an average Al content of only ~ 7%, the etching speed should be similar for p-GaN and p-AlGaN/GaN SLs samples. As shown in Fig. 4, linear fitting (broken line) can be expected from these data points. There is an offset for d_E which may refer to unstable etching condition in the initial stage or due to the existence of oxidized layer at the surface.

The influence of contact layers was then carefully investigated. Average Mg concentration measured by SIMS was 1.3 × 10^{19} cm^{-3} for bulk p-AlGaN/GaN SLs, which is quite uniform except the very initial stage and near the surface as shown in Fig. 5(a). Since Hall measurements are used for the evaluation of uniform layers, the thickness of actual conductive layer (d_C) with a uniform hole concentration should be determined carefully. Owing to the delay of doping, d_C is obviously smaller than Mg doped layer thickness (d_{Mg}). The period thickness of p-AlGaN/GaN SLs was measured by high-resolution X-ray diffraction (HR-XRD) and fitted to be 4.99 nm (Fig. 7). So, the total thickness of p-AlGaN/GaN SLs was 499 nm, which was similar to our designed thickness. Since the contact layer was 24 nm-thick, d_{Mg} was calculated to be 523 nm.

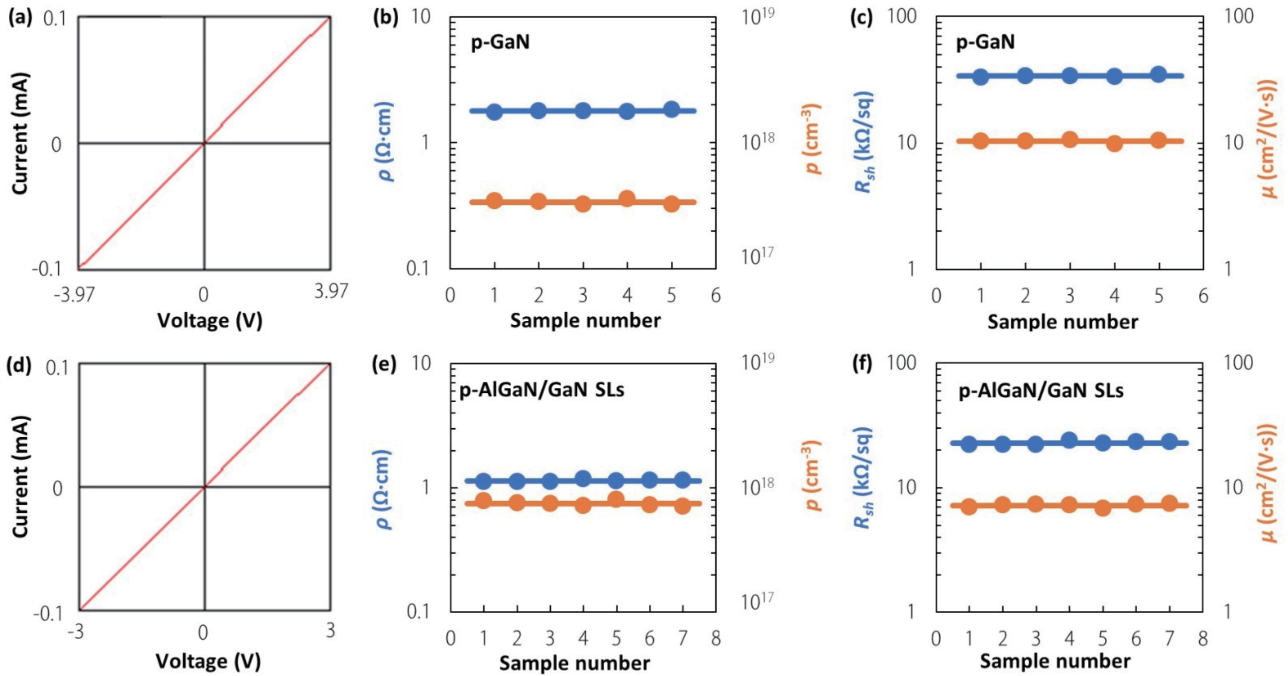

Fig. 2. (Color online) (a) Typical *I–V* curve, (b) ρ and p, (c) R_{sh} and μ results for p-GaN samples. (d) Typical *I–V* curve, (e) ρ and p, (f) R_{sh} and μ results of p-AlGaN/GaN SLs samples.

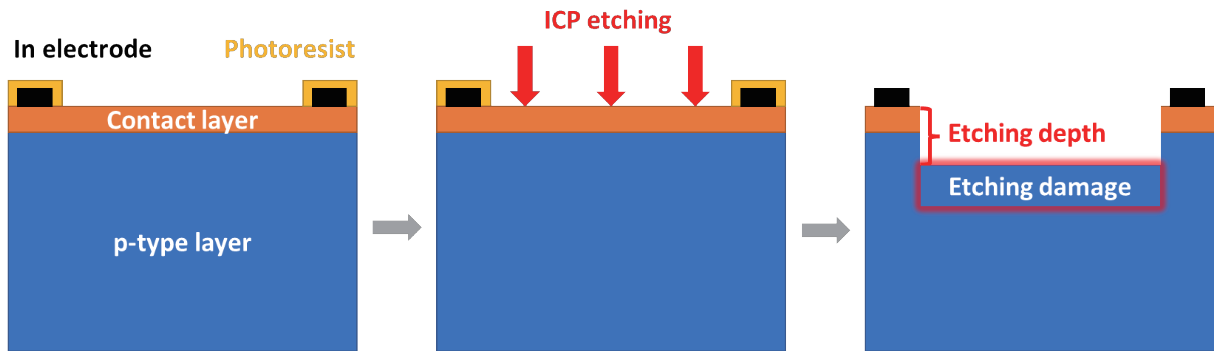

Fig. 3. (Color online) Schematic of step etching experiment, etching damage is also considered.

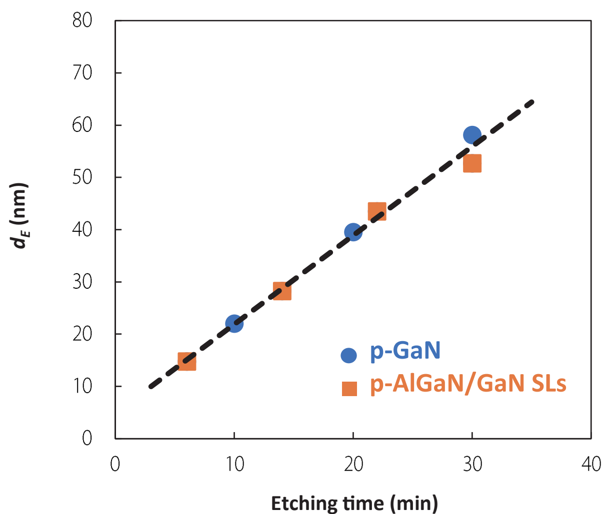

Fig. 4. (Color online) Measured d_E by AFM for different etching time.

The band diagram near the fresh p-InGaN/p+-GaN surface is simulated in Fig. 6(b). The surface depletion width is mainly determined by the acceptor concentration and the barrier height at the surface. Owing to the strong spontaneous and piezoelectric polarization effect and lowed barrier height of InGaN, the valence band is tilted upward and the depletion width is 5 nm. Assuming the Fermi-level stabilization energy, the valence band at the surface is located at −2.22 eV for $In_{0.2}Ga_{0.8}N$[19], the electric field in p-$In_{0.2}Ga_{0.8}N$ layer is calculated to be 3.4 MV/cm[20, 21] and the conduction-to-valence-band offset ratio of InGaN/GaN interface is assumed as $\Delta E_C : \Delta E_V = 60 : 40$[22] in the simulation. The SIMS data for the surface region is usually not so reliable due to surface contamination, thus a designed profile is assumed instead as shown in Fig. 5(b). As the Mg concentration near the surface increases to approach ~ 1×10^{20} cm^{-3}, the hole concentration tends to decrease due to self-compensation when Mg concentration is above 4×10^{19} cm^{-3}, which has been examined through our separate study. Here it should be pointed out that the highly doped layer near the surface does not necessarily imply higher conduction, but its resistivity tends to stay nearly the same or even becomes higher due to self-compensation. However, it still has a prominent effect to reduce the depletion width at the surface, facilitating the ohmic contact. The equivalent depth where uniform conduction starts (d_C^S) is calculate to be 5 nm considering the expected hole dis-

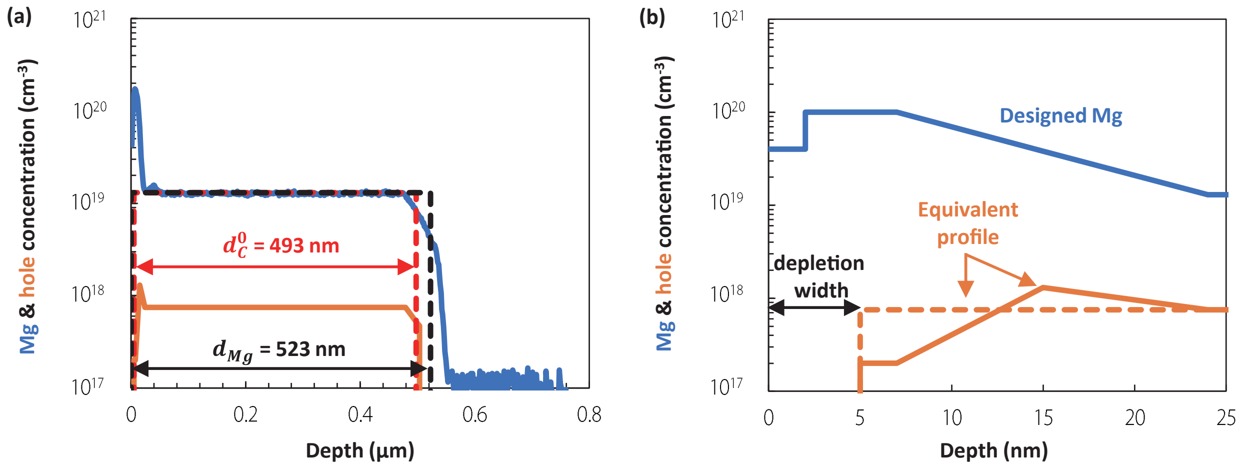

Fig. 5. (Color online) (a) Measured Mg & hole concentration for p-AlGaN/GaN SLs sample. The red broken line shows the equivalent doping profile used in the Hall measurements. (b) Analyzed Mg & hole concentration near the surface region for the same sample. The orange broken line shows the equivalent hole profile with a constant density.

Fig. 6. (Color online) (a) Fitting of d_{NC} with different d_E. (b) Band diagram near the fresh surface. (c) Band diagram near the etched surface when contact layers are completely removed. (d) Measured R_{sh} plotted against d_C.

tribution near the surface. Same method is applied to determine the equivalent depth where uniform conduction ends near the starting position of Mg-doping (d_C^e), and d_C^e is calculated to be 498 nm. As a result, the effective conductive layer thickness with a uniform hole concentration before etching (d_C^0) is 493 nm.

4 samples marked as A1 to A4 were selected from previous 7 p-AlGaN/GaN SLs samples. The ICP etching time was varied as 6, 14, 22, 30 min for A1, A2, A3 and A4, respectively. Then, d_E could be calculated easily through the fitting curve

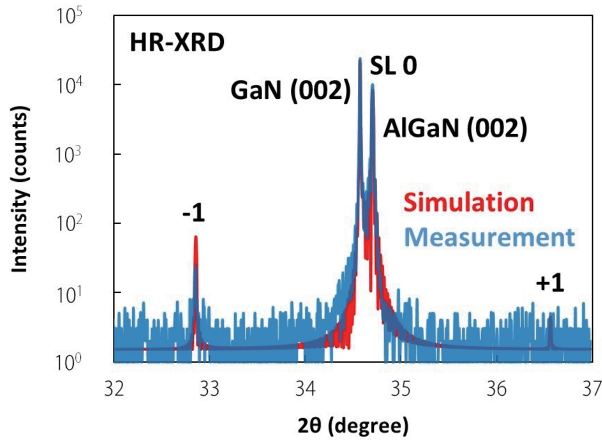

Fig. 7. (Color online) The 2theta/omega scan of p-AlGaN/GaN SLs by HR-XRD (Bruker D8 Discover).

in Fig. 4. As we know, ρ can not be measured accurately if the thickness is not certain. However, R_{sh} which can be measured accurately without the knowledge of layer thickness. R_{sh} will definitely increase due to the decrease of d_C after etching. The change of R_{sh} before and after different etching time could be fitted to give the thickness of non-conductive layer near the etched surface (d_{NC}) consisting of a damage layer and an associated depletion layer, as can be written in Eqs. (1) and (2).

$$R_{sh} = \frac{d_C^0}{d_C} \cdot R_{sh}^0, \tag{1}$$

$$d_C = d_C^e - d_E - d_{NC}, \tag{2}$$

where R_{sh}^0 is the average sheet resistivity before etching.

Fig. 6(a) shows the R_{sh} after etching. The solid line, broken line and dotted line are the fitted ones using R_{sh} expressed by Eqs. (1) and (2) with d_{NC} set to 0, 28 and 50 nm, respectively. It should be noted that d_{NC} could increase with increasing etching time. However, a constant value of d_{NC} = 28 nm also gives us a reasonable fitting in Fig. 6(a) and is used in the subsequent calculation. The band diagram of etched surface when contact layers are completely removed is also simulated in Fig. 6(c). Here, p-$Al_{0.14}Ga_{0.86}N$/GaN SLs is simplified as p-$Al_{0.07}Ga_{0.93}N$ single layer. The valence band at the surface is positioned at –2.56 eV for $Al_{0.07}Ga_{0.93}N$[19]. The depletion width is estimated to be 15 nm so that the etching damage depth is regarded as 13 nm. Then, d_C can be calculated properly and the electrical properties can be determined accurately in the Hall measurements using these d_C values. In Fig. 6(d), measured R_{sh} values including both non-etched and etched samples are plotted against estimated d_C. R_{sh} is inversely proportional to d_C, which is indicative of assumed uniform doping. This result should justify our treatment to estimate d_C. d_{Mg} implies the designed thickness of Mg-doped layer. The effective thickness d_C is smaller than d_{Mg} because of the etching depth, surface and sub/epi interface depletion width, Mg doping-delay, damaged width, and the p^+ layer carrier profile.

P-GaN samples were also analyzed using the same method and results are added in Fig. 8 together with p-AlGaN/GaN SLs. The solid and broken lines and the data points at 0 nm in

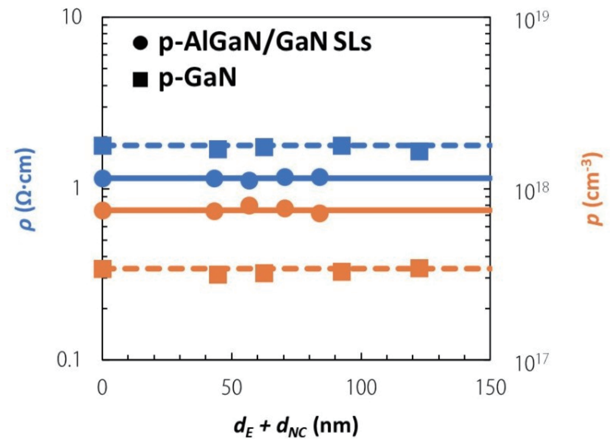

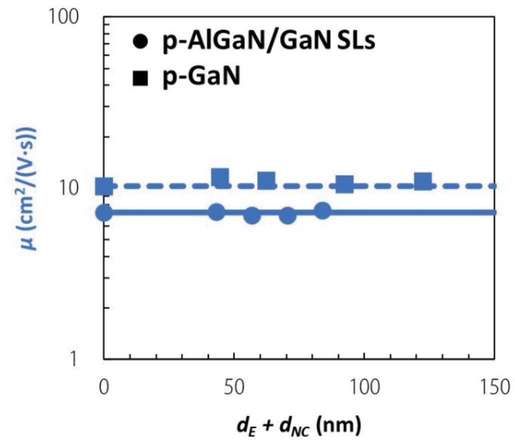

Fig. 8. (Color online) Electrical properties of p-AlGaN/GaN SLs (circles) and p-GaN (squares) samples before and after ICP etching. Solid and broken lines are the average value before etching for p-AlGaN and p-GaN, respectively.

Fig. 8 are the average values before etching. It is clear that the measured values of ρ, μ and p remain almost identical before and after etching. The contacting scheme is experimentally proven to be suitable and practical. The electrical properties of AlGaN/GaN SLs are summarized as shown in Table 1.

Since it is obvious that 2 nm p-InGaN is quite thin and exists within the depletion width, this p-InGaN/p^+-GaN hetero-interface will have no significant effect on the bulk electrical properties while improving the contact properties. This contacting scheme to Pd-based metal has also been studied in our previous work[23], exhibiting a relatively low specific contact resistivity of 4.9×10^{-5} Ω·cm^2 @ $J = 3.4$ kA/cm^2.

The determined difference between d_C and d_{Mg} is ~ 30 nm for unetched sample in this study. For convenience, this value is recommended for similar p-type structures in practice. If the sample structure is known, d_C can be calculated by the method described in this paper, and one can certainly improve the accuracy.

4. Conclusions

Quick and accurate Hall-effect measurements for GaN-based p-type layers were established by using suitable p-$In_{0.2}Ga_{0.8}N$ (2 nm)/p^+-GaN (22 nm) contacting scheme with In balls after optimizing annealing condition. The electrical properties of both p-GaN and p-AlGaN/GaN SLs samples were evaluated and the standard deviation of each value was ~ 3% and ~ 4%, respectively. The thickness of non-conductive surface lay-

Table 1. The detailed electrical properties of AlGaN/GaN SLs samples.

Parameter	ρ (Ω·cm)	μ ($cm^2/(V\cdot s)$)	p (cm^{-3})	R_{sh} (kΩ/sq)	d_C (nm)	Etching
A1 – A4 (average)	1.16	7.23	7.49×10^{17}	23.4	493	No
A1	1.16	7.31	7.39×10^{17}	24.9	455	Yes
A2	1.12	6.95	8.03×10^{17}	25.9	441	Yes
A3	1.17	6.95	7.66×10^{17}	27.4	428	Yes
A4	1.18	7.40	7.18×10^{17}	28.3	414	Yes

er was estimated to be ~ 28 nm for the etched samples and the etching damage was estimated to be ~ 13 nm. Identical values could be obtained before and after the removal of contact layer when reasonable conducive layer thickness was used.

Acknowledgements

This work was financially supported by the National Key Research and Development Program of China (2017YFE0131500), the Key Research and Development Program of Guangdong Province (2020B090922001), National Natural Science Foundation of China (61834008, 62150710548), Key Research and Development Program of Jiangsu province (BE2020004, BE2021008-1), Guangdong Basic and Applied Basic Research Foundation (2019B1515120091). We are thankful for the technical support from Nano Fabrication Facility, Platform for Characterization & Test, and Nano-X of SINANO, CAS.

References

[1] Amano H, Kito M, Hiramatsu K, et al. P-type conduction in Mg-doped GaN treated with low-energy electron beam irradiation (LEEBI). Jpn J Appl Phys, 1989, 28, L2112
[2] Nakamura S, Mukai T, Senoh M, et al. Thermal annealing effects on P-type Mg-doped GaN films. Jpn J Appl Phys, 1992, 31, L139
[3] Kumakura K, Kobayashi N. Increased electrical activity of Mg-acceptors in $Al_xGa_{1-x}N$/GaN superlattices. Jpn J Appl Phys, 1999, 38, L1012
[4] Kumakura K, Makimoto T, Kobayashi N. Activation energy and electrical activity of Mg in Mg-doped $In_xGa_{1-x}N$ (x < 0.2). Jpn J Appl Phys, 2000, 39, L337
[5] Nakarmi M L, Kim K H, Li J, et al. Enhanced p-type conduction in GaN and AlGaN by Mg-δ-doping. Appl Phys Lett, 2003, 82, 3041
[6] Iida D, Tamura K, Iwaya M, et al. Compensation effect of Mg-doped a- and c-plane GaN films grown by metalorganic vapor phase epitaxy. J Cryst Growth, 2010, 312, 3131
[7] Kinoshita T, Obata T, Yanagi H, et al. High p-type conduction in high-Al content Mg-doped AlGaN. Appl Phys Lett, 2013, 102, 012105
[8] Tian A Q, Liu J P, Ikeda M, et al. Conductivity enhancement in AlGaN: Mg by suppressing the incorporation of carbon impurity. Appl Phys Express, 2015, 8, 051001
[9] Yang J, Zhao D G, Jiang D S, et al. Different variation behaviors of resistivity for high-temperature-grown and low-temperature-grown p-GaN films. Chin Phys B, 2016, 25, 027102
[10] Narita T, Tomita K, Tokuda Y, et al. The origin of carbon-related carrier compensation in p-type GaN layers grown by MOVPE. J Appl Phys, 2018, 124, 215701
[11] Kim J K, Lee J L, Lee J W, et al. Low resistance Pd/Au ohmic contacts to p-type GaN using surface treatment. Appl Phys Lett, 1998, 73, 2953
[12] Kumakura K, Makimoto T, Kobayashi N. Ohmic contact to *p*-GaN using a strained InGaN contact layer and its thermal stability. Jpn J Appl Phys, 2003, 42, 2254
[13] Li Z C, Huang R, Chen X, et al. The significant effect of carbon and oxygen contaminants at Pd/p-GaN interface on its ohmic contact characteristics. Phys Status Solidi A, 2021, 218, 2000603
[14] Ho J K, Jong C S, Chiu C C, et al. Low-resistance ohmic contacts to p-type GaN achieved by the oxidation of Ni/Au films. J Appl Phys, 1999, 86, 4491
[15] Chen L C, Chen F R, Kai J J, et al. Microstructural investigation of oxidized Ni/Au ohmic contact to *p*-type GaN. J Appl Phys, 1999, 86, 3826
[16] Ikeda M, Uchida S. Blue-violet laser diodes suitable for blu-ray disk. Phys Stat Sol (a), 2002, 194, 407
[17] Kumabe T, Ando Y, Watanabe H, et al. Etching-induced damage in heavily Mg-doped p-type GaN and its suppression by low-bias-power inductively coupled plasma-reactive ion etching. Jpn J Appl Phys, 2021, 60, SBBD03
[18] Kent D G, Lee K P, Zhang A P, et al. Effect of N_2 plasma treatments on dry etch damage in n- and p-type GaN. Solid State Electron, 2001, 45, 467
[19] Walukiewicz W, Li S X, Wu J, et al. Optical properties and electronic structure of InN and In-rich group III-nitride alloys. J Cryst Growth, 2004, 269, 119
[20] Bernardini F, Fiorentini V. Spontaneous versus piezoelectric polarization in III-V nitrides: Conceptual aspects and practical consequences. Phys Stat Sol (b), 1999, 216, 391
[21] Fiorentini V, Bernardini F, Ambacher O. Evidence for nonlinear macroscopic polarization in III-V nitride alloy heterostructures. Appl Phys Lett, 2002, 80, 1204
[22] Zhang F, Ikeda M, Zhou K, et al. Injection current dependences of electroluminescence transition energy in InGaN/GaN multiple quantum wells light emitting diodes under pulsed current conditions. J Appl Phys, 2015, 118, 033101
[23] Zhang M L, Ikeda M, Huang S Y, et al. Ni/Pd-based ohmic contacts to p-GaN through p-InGaN/p^+-GaN contacting layers. J Semicond, 2022, 43, 092803

Siyi Huang got his bachelor's degree in 2011 from University of Science and Technology Beijing and his master's degree in 2014 from City University of Hong Kong. Now he is a doctoral student at University of Science and Technology of China under the supervision of Prof. Masao Ikeda and Prof. Jianping Liu. His research focuses on MOCVD growth and characterization of GaN-based materials.

Masao Ikeda received his doctoral degree from Waseda University, Tokyo, Japan, in 1991. He is currently a Professor with the Suzhou Institute of Nano-Tech and Nano-Bionics, Chinese Academy of Sciences, Suzhou, China. His current research interests include III–V compound semiconductor materials and devices.

Jianping Liu is a professor in Suzhou Institute of Nano-Tech and Nano-Bionics, Chinese Academy of Sciences. He earned his doctoral degree from Institute of Semiconductors, Chinese Academy of Sciences in 2004. He worked at Lab of Optoelectronics Technology at Beijing University of Technology from 2004 to 2006. He did postdoctoral research in Department of Electrical Engineering at Georgia Institute of Technology from 2006 to 2010. His research interests include MOCVD growth, GaN-based materials and devices.